Universe Scientific Publishing

ORIGINAL ARTICLE

Influence of mete ocean processes on MSYM sea level predictions in the Malacca Straits

Sofia Bartolomeu[1], Madalena S. Malhadas[1,2], João Ribeiro[1], Paulo C. Leitão[1], João M. Dias[3]

[1] Hidromod Lda. - Modelação em Engenharia, Lda. Rua Rui Teles Palhinha, nº 4, 1º. 2740-278, Porto Salvo, Portugal

[2] DHI Water & Environment (S) Pte Ltd. 1 Cleantech Loop, #03-05 CleanTech One, Singapore 637141

[3] Departamento de Física, CESAM, Universidade de Aveiro, Campus Universitário de Santiago 3810-193 Aveiro, Portugal

Abstract: The South China Sea region, and particularly the Malacca and Singapore Straits, are known by the complex tidal dynamics, which is influenced by the tidal propagation from Pacific and Indian Oceans. In spite of the dynamic complexity, the region is very relevant economically, especially concerning the growing oil drilling activities. To give support to accidental oil spill prevention and response, an operational oil spill forecast system was developed for the Strait of Malacca. The hydrodynamic system validation revealed good results, in general. However, besides all the modeling efforts, some discrepancies between observed and predicted sea levels were identified, mainly during neap tide and for specific tide-gauges. Therefore, the main aim of this study consists in researching the origin of these discrepancies by comparing predictions with available data and exploring their relation with the MeteOcean processes of the region. Initially sea level data for eight tide gauges was explored to get a general overview of the local tidal dynamics, and then the model performance for astronomic tide was assessed. Analysis of meteorological tides was also performed for three tide-gauges located in the Singapore and Malacca Strait, which are under the influence of the northeast or southwest monsoons. The results show that the differences between the observed and predicted sea levels in Singapore Strait are usually due to discrepancies in the meteorological tide induced by the surface wind stress acting over the Taiwan-Singapore axis, while in the Malacca Strait are mainly related with model limitations in reproducing the astronomical tide.

Keywords: tidal harmonics; sea level rise; hydrodynamic modelling; south china sea; Malacca and Singapore Strait

1. Introduction

The regions of the South China Sea, Malacca Strait and Singapore Strait are characterized by complex tidal dynamics (Akdag, 1996), entangled with the co-oscillating nature of the tide from the Pacific and Indian Ocean, mainly in response to the geometric configuration of the area. The combination of these elements with the existence of many islands and small passages, could give an estimate/overview of the complexity of the tides in the study area and the coastal water's response to various forcing mechanisms that provide the energy and momentum to drive the coastal processes.

During the past decade, numerical ocean models have been able to predict the coastal and oceanic processes with the necessary resolution to reproduce the small-scale details not captured by the observations. This level of understanding reveals itself useful for such areas as coastal engineering, fisheries, marine environment or oceanography (Wei *et al*.,

doi: 10.18686/mmf.v2i2.1069

2010). In particular, the Malacca and Singapore Straits are important economic regions characterized by an intense maritime navigation traffic dependent on local tidal dynamics, requiring the development of accurate ocean models.

Singapore has a significant importance within global shipping routes, and with the increase in shipping and port activities the marine environmental protection of the Singapore Strait has become more and more critical (Chen *et al*., 2010).

The Malacca Strait is one of the most important shipping routes in the world and is a canal between the Indian and Pacific Oceans, connecting three different countries with a large population: India, Indonesia and China (Rizal *et al*., 2010). Additionally, there has been an expansion of the oil drilling activity in this region, which is likely to increase in the next few years, as new oil deposits are being discovered. As a consequence, oil spills are now considered an important hazard that might become more frequent in the Malacca Strait (Camerlengo and Demmler, 1997). Therefore, the different aspects of removal and containment of oil spills under adverse weather conditions will necessarily have to undergo an accelerated expansion in the foreseeable future.

The needs from marine environmental protection and accidental oil spill protection measures lead to a former application of a trajectory model integrated with remote sensing data in a Geographic Information System (GIS) (Assilzadeh *et al*., 1999) and to the development of accurate numerical models not only for Malacca, (e. g., Rizal *et al*., 2010), but also for Singapore (Tkalich *et al*., 1999; Wei *et al*., 2010). In this context, the MSYM model was developed as an operational oil spill forecast system for the Strait of Malacca (www.hidromod.pt). It integrates appropriate hydrodynamic and oil dispersion models, which were developed to provide predictions of the movement, dispersion and trajectory, shore reach and impact of pollutants on the coastal area and marine structures. The solution proposed make use of the AQUASAFE server (www.aquasafeonline.net/) to manage the information and MOHID (www.mohid.com) to compute the hydrodynamic and oil spills transport and dispersion. MOHID is an integrated water modelling platform that can be used to simulate the dynamics of water bodies, porous media flow and infiltration, and watersheds, which has been used to simulate a variety of physical, chemical and ecological processes at different scales in marine systems. Over the past years, with a continuous development of new features, MOHID Water has been applied to several coastal and estuarine areas worldwide and has shown its ability to simulate complex features of the flows. MOHID has been intensively applied to the Portuguese coast, including the main estuaries and coastal lagoons, like Aveiro (e. g., Vaz *et al*., 2008), Tagus Estuary (Braunschweig *et al*., 2003), Portuguese Monte Novo, Roxo and Alqueva reservoirs (Braunschweig, 2001), most of the Galician Rías (e. g., Montero *et al*., 1999; Martins *et al*., 2001; Villarreal *et al*., 2002), and other European estuaries (Leitão, 1996).

The first validation work conducted for the model implemented for the Strait of Malacca revealed, in general, a good fit between seal level observations and model predictions. However, there are some particular locations under important dynamic ocean and meteorological processes where the discrepancies are high, independently of the modelling efforts performed to improve the results. It is important to understand the reasons for these inaccuracies, mainly associated with the neap tide, so that model predictions can be improved. Thus, this work aims to deeply validate at different levels the MSYM model for the sea level, including the regions of South China Sea, Malacca and Singapore Straits, and to understand the reasons behind the highest discrepancies between observed and predicted sea level in light of the analysis of the main dynamic processes acting over the region (e. g. wind speed and direction).

2. Study Area

In **Figure 1** is represented the location and bathymetry of the study area. Its analysis reveals that the coastal areas of this region are relatively shallow and that the bathymetry of the Malaysia Peninsula's eastern continental shelf has a moderate slope which progressively extends towards the South China Sea. This is the largest semi-enclosed marginal sea in the tropics, from 0^{o}–23^{o} N and 99^{o}–121^{o} E, surrounded by the Asian mainland and wider than 1100 km, and dominated by diurnal and mixed tides. It is composed by a deep central basin and two extensive continental shelves with mean water depth of approximately 1800 m. The main topographic characteristic of the oceanic regions in the

northern and central parts of the South China Sea is a V-shaped basin (Akdag, 1996), with a maximum depth higher than 5400 m.

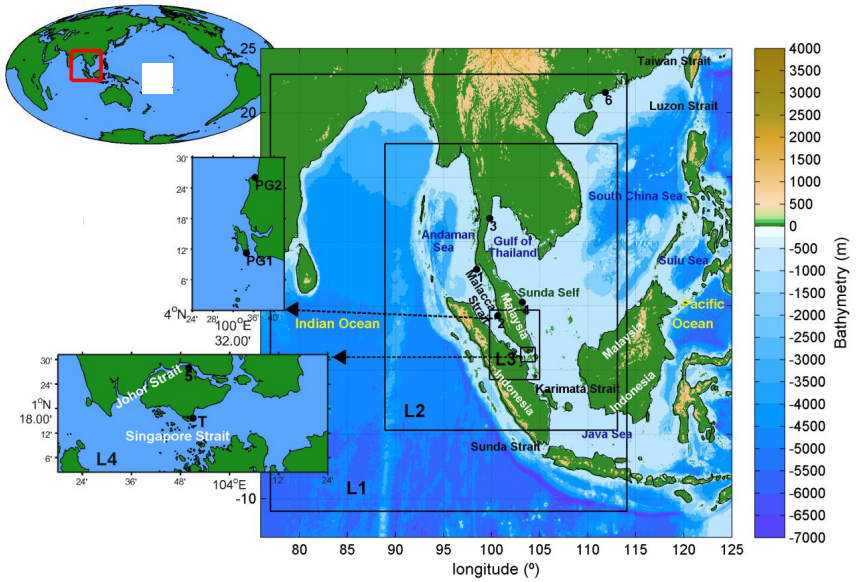

Figure 1; Location and bathymetry of study area. It includes the location of the tide gauges from Global Sea Level Observing System (GLOSS) numbered by 1 – Ko Taphao Noi; 2 – Pengalan; 3 – Ko Lak; 4 – Kuala Terengganu; 5 – Singapore; 6 – Zhapo; from the Marine Electronic Highway (MEH) by "T" and from the Hydraulic-Environmental-Civil Engineering Company (HYDEC) by PG1 and PG2. It also contains the nested configuration for the Malacca and Singapore Straits of the MSYM model (map A: Level 1 (L1); Level 2 (L2); Level 3 (L3) and Level 4 (small square-amplified in map B)). The map A used the bathymetry data from the 1-minute Global Gridded Elevation Data, ETOPO1, of the National Geophysical Data Center.

The Malacca Strait is mainly characterized by a semidiurnal tidal pattern, and is composed by a channel with a complex topography, between the Malaysia Peninsula and Sumatra, linking the Indian Ocean and Andaman Sea (at the North) to the South China Sea (at the South). Its south connection is a channel named Singapore Strait that extends for 105 km and where the water depth ranges between 30 and 120 m. It is influenced by the interactions between the Indian (mainly semidiurnal) and Pacific Oceans (mainly diurnal) having a complex tidal pattern that also results from the tidal propagation along a complex coastline geometry, with small islands and sharply varying bathymetry.

Regarding to the weather conditions, the interannual variability of temperatures associated with El Niño modulates the atmospheric forcing of the ocean in the equatorial Pacific, causing the highest changes in equatorial dynamics (Stewart, 2008). Therefore, changes in sea level are directly linked to a number of atmospheric and oceanic processes. Additionally, the Asian monsoons (northeast (NE) from November to March, and southeast (SW) from May to September (Wang *et al*., 2001)) greatly affect the circulation of the entire region (bounded by Gulf of Thailand on the north, Karimata Strait on the south, east coast of Peninsular Malaysia on the west, and break of the Sunda Shelf on the east). These act essentially over the region of the South China Sea and tend to induce positive or negative sea level anomalies (SLA's) in the Singapore Strait (Tkalich *et al*., 2013; Choon *et al*., 2006; Chen *et al*., 2011). According to Azmy *et al*. (1991) the pile up of water during the winter monsoon is greater than the lowering of the sea level during the summer monsoon. If strong sea level surges during NE monsoon coincide with spring tide, they usually lead to coastal floods in the region. Following its high relevance, storm surge, monsoons and several constituents of the circulation in Singapore Strait Region have been studied by several oceanographers (Camerlengo and Demmler, 1997; Choon *et al*., 2006; Chen *et al*., 2010, 2010b; Kurniawan *et al*., 2011; Tkalich *et al*., 2012, 2013).

The monsoonal effects are not severe in the Malacca Strait because of the sheltering effect of the Malaysia Peninsula and of the island of Sumatra. Indirectly, however, the monsoon seasons greatly influence the circulation in the strait, where are found two rainy seasons of unequal magnitude without any really dry period between (Keller and Richards, 1967).

3. Methodology and data

The MOHID model was used in this study to compute sea level, with the aim of validating the model and studying the storm surge effects in this area. This hydrodynamic model has been configured to be applied in the Strait of Malacca - the MSYM model.

3.1 Model's configuration for the Malacca Strait (MSYM)

The MSYM adopts a downscaling approach using four levels of grid nesting (Level 1 to Level 4) with different dimensions and horizontal resolutions (**Figure 1**). The first domain includes the West Indian Ocean and part of the South China Sea; the second domain includes the Andaman Sea and part of the South China Sea; the third domain includes the Malacca Strait and finally the fourth domain includes the Singapore Strait. One-way nesting is used, in which only the large-scale models influence the local models. At this stage, all the levels are 2D-H barotropic, using only 1 sigma layer in the vertical dimension. The MSYM model application simulates the sea level and the currents for all domains with a time step of 240 s, for the first domain, 120 s for the second and third domains and 30 s for the fourth domain. Table 1 summarizes the main characteristics of the implemented model configuration for the Malacca Strait.

	Level 1	**Level 2**	**Level 3**	**Level 4**
Domain	West Indian Ocean and South China Sea	Andaman and South China Sea	Malacca Strait	Singapore Strait
Grid Corners	lon: 77.0º to 114.1º lat: 23.0º to -11º	lon: 88.9º to 113.1º lat: 17.6º to -4.7º	lon: 99.8º to 105.0º lat: 4.65º to -0.75º	lon: 103.3º to 104.4º lat: 1.52º to 1.04º
Dimension/Nº of Cells	371x340/126140	483x445/214935	524x539/282436	540x240/129600
Δx (º)	0.089	0.044	0.0089	0.0018
Δt (s)	240	120	120	30
Horizontal eddy viscosity	100 m^2s^{-1}	50 m^2s^{-1}	10 m^2s^{-1}	2 m^2s^{-1}
Vertical Discretization	1 sigma layer	1 sigma layer	1 sigma layer	1 sigma layer
Simulated Properties	Sea level and current velocities	Sea level and current velocities	Sea level and current velocities	Sea level and current velocities
Open Boundary Condition	Tidal global solution (FES2004)	Level 1+Inverted Barometer	Level 2	Level 3
Surface Boundary Condition	-	Wind and atmospheric pressure	Wind and atmospheric pressure	Wind and atmospheric pressure

Table 1. Main characteristics of the nested models configuration for MSYM

The first domain (L1) has a horizontal resolution of about 10 km encompassing a larger area. This grid data domain is coarse, since the goal is to simulate large-scale processes (e.g., tide). In the open boundary of Level 1, a sea level interpolated from the FES2004 global tidal solution (Lyard *et al.*, 2006) was imposed. Zero free surface gradient and zero velocity at all grid points were used as initial conditions. The second domain (L2) is regional, and has a horizontal resolution of about 5 km. The open boundary conditions for this level were defined by adding the inverted barometer effect (sea level variation due to pressure gradients) to the solution of Level 1 (high frequency). The surface boundary condition for wind stress and atmospheric pressure is applied by using the Global Forecast System of the National Oceanic and Atmospheric Administration (GFS NOOA) weather prediction solution. The third domain (L3) comprises the Malacca Strait with a horizontal resolution of about 1 km. The fourth domain (L4) is local and includes the Singapore Strait with a 200 m (0.0018º) horizontal resolution. The open boundary conditions for levels 3 and 4 are prescribed from the upper levels, and meteorological forcing (wind and atmospheric pressure) are still being applied

using the GFS solution.

3.2 Simulations

Table 2 summarizes the simulations performed during this study, indicating the time interval, the validated area, the tidal forcing and analysed levels. Three simulations were performed. The first is a single four-nested MSYM run (Level 1, 2, 3 and 4) only forced by the astronomic tide and all levels were analysed. The second and third runs use astronomic tide and meteorological forcing from GFS-NOAA solution (wind and the atmospheric pressure), and the difference between them consists in the time interval and the domain analysed: Levels 4 and 3, respectively. The hydrodynamic model was spun up from rest over three days (not included in the aforementioned periods).

Simulated period	**Validated Area**	**Forcing**	**Analysed Levels**
17/12/1988 to 23/12/1989	South China Sea and Andaman Sea	Astronomic tide	L1, L2, L3 L4
24/11/2012 to 6/04/2013	Singapore Strait	Tidal and meteorological GFS-NOAA forcing	L4
5/4/2010 to 19/4/2010	Pangkor	Tidal and meteorological GFS-NOAA forcing	L3

Table 2. Simulations considered: period, area, tidal forcing and analysed levels

3.3 Data Source

In order to validate the predicted sea levels, a total of nine tide-gauges stations were considered (**Figure 1**). Table 3 displays the coordinates and levels where each tide-gauge was included, as well as the available observed sea level data and the missing data. The data gaps vary from a few hours to less than one month and the periods of the available data differ from station to station. The three simulations have different time intervals, following the data sources. The first time interval is the longest period of continuous data (without missing days) common to the six Global Sea Level Observing System (GLOSS) tide-gauges: Ko Taphao Noi (number 1 in **Figure 1**), Pengkalan (2), Ko Lak (3), Kuala Terengganu (4), Singapore (5) and Zhapo (6). The second time interval corresponds to the available observed sea level provided by the Marine Electronic Highway Project (MEH) for Tanjong Pagar (marked by T), in the Singapore Strait. The third time interval is related with the available observed data of the Hydraulic-Environmental-Civil Engineering Company under an engineering project (HYDEC) for the tide-gauges of Pangkor (located with TG1 and TG2). The stations are located in coastal waters systems with different characteristics: Ko Taphao Noi and Kuala Terengganu stations are located on a coastal water system; Pengalan, Zhapo and PG1 stations are located on a estuarine system; Ko Lak and PG2 stations are located on a bay system; Singapore is on the Johor Strait and Tanjong Pagar station is on the Singapore Strait.

Sources	**Stations**	**Lat.**	**Lon.**	**MSYM levels**	**Available data**	**Missing days**
GLOSS (42)	Ko Tapthao Noi	7º 50’	98º 26’	L1, L2	1/01/1985 – 31/12/2010	223
GLOSS (43)	Pengkalan	4º 14’	100º 37’	L1, L2, L3	12/12/1984 – 31/12/2006	218
GLOSS (39)	KoLak	11º 47’	99º 49’	L1, L2	1/01/1985 – 31/12/2010	483
GLOSS(293)	Kuala Terengganu	5º 16’	103º 11’	L1, L2	31/10/1984 – 31/12/2006	77
GLOSS (44)	Singapore	1º 28’	103º 50’	-	13/08/1981 – 31/08/1990	32
GLOSS (78)	Zhapo	21º 35’	111º 50’	L1	1/01/1975 – 31/12/1997	0
MEH	Tanjong Pagar	1º 16’	103º 51’	L4	24/11/2012 – 6/04/2013	24
HYDEC	Pangkor, TG1	4º 26’	100º 36’	L1, L2, L3	5th - 19th of 04/2010	0
HYDEC	Pangkor, TG2	4º 11’	100º 35’	L1, L2, L3	5th - 19th of 04/2010	0

Table 3. Coordinates of the Global Sea Level Observing System (GLOSS with respective number ID), Marine Electronic Highway Project (MEH) and the Hydraulic-Environmental-Civil Engineering Company Project (HYDEC)

tide-gauges used with the respective available data

Moreover, the sample interval is different according to the source of the tide-gauge: 1 hour, 30 minutes and 10 minutes for GLOSS, MEH and HYDEC tide-gauges, respectively. It is important to note that the Tanjong Pagar tide-gauge is located on the Singapore Strait, and is included only in the L4 domain (due to resolution constraints) of the MSYM model.

3.4 Methods

The analysis performed in this study was divided into three main parts. First it was analysed the sea level for each tide-gauge, including a monthly sea level anomalies analysis. In the second part, the accuracy of the MSYM in predicting the astronomic tide was assessed, computing and comparing the amplitude and phase of the main harmonic constituents for model predictions and observed sea level. In the last part, it was investigated the sea level anomalies, the storm surges. In general, the occurrence of storm surges induces a higher discrepancy between observations and predictions. In this part, it is explored the origin of these discrepancies researching their relation with the MeteOcean processes occurring in the straits.

For these analysis was applied several techniques, parameters and error measures. The harmonic method applied in this work is the t_tide function which separates the tidal and non-tidal energies (Pawlowicz *et al.*, 2002). The astronomic tide was assessed comparing the amplitude and phase of the main constituents given by the harmonic analysis (considering the harmonics produced by FES2004 - used by the MSYM model as boundary conditions): Semidiurnal (N_2, M_2, S_2, K_2), Diurnal (Q_1, O_1, P_1, K_1) and Quadridiurnal (M_4). Using the amplitude of the four main constituents - M_2, S_2, O_1 and K_1 - the Form factor (F) was also calculated by equation (1):

$$F = \frac{K_1 + O_1}{M_2 + S_2} \tag{1}$$

According to the result, the tide is classified, quantitatively, as: semidiurnal (F < 0.25, i.e. two main cycles per day); mixed mainly semidiurnal (0.25 < F < 1.5); mixed dominantly diurnal (1.5 < F < 3.0); diurnal (F > 3.0, i.e. one cycle per day).

On the other hand, the meteorological tide was subjected to spectral analysis (to found the frequencies with higher amplitude), and was also compared with concurrent wind (speed and direction) and atmospheric pressure for the region.

Some error measures, to compare observed and predicted data, were also calculated: the centred pattern of Root Mean Squared Error difference (RMSE', equation 2), the Correlation coefficient, the anomalous pattern correlation between predictions and observations (R, equation 3) and the Relative Error (equation 4). In these equations, f are predictions, r are observations, n is the total number of points in a temporal or spatial domain or spatial-temporal combined space and σ_f and σ_r represent the variances of f and r, respectively.

$$RMSE' = \sqrt{\frac{1}{n}\sum_{i=1}^{} [(f_n - \bar{f}) - (r_n - \bar{r})]^2} \tag{2}$$

$$R = \frac{1}{n}\sum_{i=1}^{} \frac{(f_n - \bar{f}).(r_n - \bar{r})}{\sigma_f \sigma_r} \tag{3}$$

$$\text{Relative Error}(\%) = \frac{RMSE'}{4\sigma_r} \times 100 \tag{4}$$

Finally, to compare the results (amplitude and phase) of each harmonic constituent i, the Mean Complex Amplitude Error (HC) was computed (equation 5), where $,_{mod}$, h_{obs}, φ_{mod} and φ_{obs} are amplitudes and phases determined from predictions and observations, respectively (Chanut *et al.*, 2008), as well as the Relative Mean complex amplitude error (Relative HC), equation 6:

$$HC_i = \left\{\left[h_{mod_i}\cos\left(\Phi_{mod_i}\right) - h_{obs_i}\cos\left(\Phi_{obs_i}\right)\right]^2 + \left[h_{mod_i}\sin\left(\Phi_{mod_i}\right) - h_{obs_i}\sin\left(\Phi_{obs_i}\right)\right]^2\right\}^{\frac{1}{2}} \tag{5}$$

$$\text{Relative } HC_i = \frac{HC_i}{h_{obs_i}} \times 100 \tag{6}$$

4. Results and Discussion

The first part of this section is focused in a general analysis of the sea level for the available tide-gauges, followed by the study of the astronomic and the meteorological tides. For that, observations were compared with the MSYM predictions to identify the higher differences and explore their origins.

4.1 Sea level analysis

Aside from the co-oscillating nature of the tide from the Pacific and Indian Ocean, which is modified by the monsoon of the region and by the local geomorphology, the characteristics of the sea level (for both the astronomic and the meteorological tides) are different for each tide-gauge under analysis. From **Figure 2** it is clear that the amplitude of the astronomic tide (represented in dark blue/black) is highest in Zhapo, followed by the stations located in the Malacca Strait (Ko Taphao Noi and Pengkalan) and in the Singapore Strait (Singapore and Tanjong Pagar). Conversely, the tide-gauges in Ko Lak and Kuala Terengganu present the lowest tidal amplitudes.

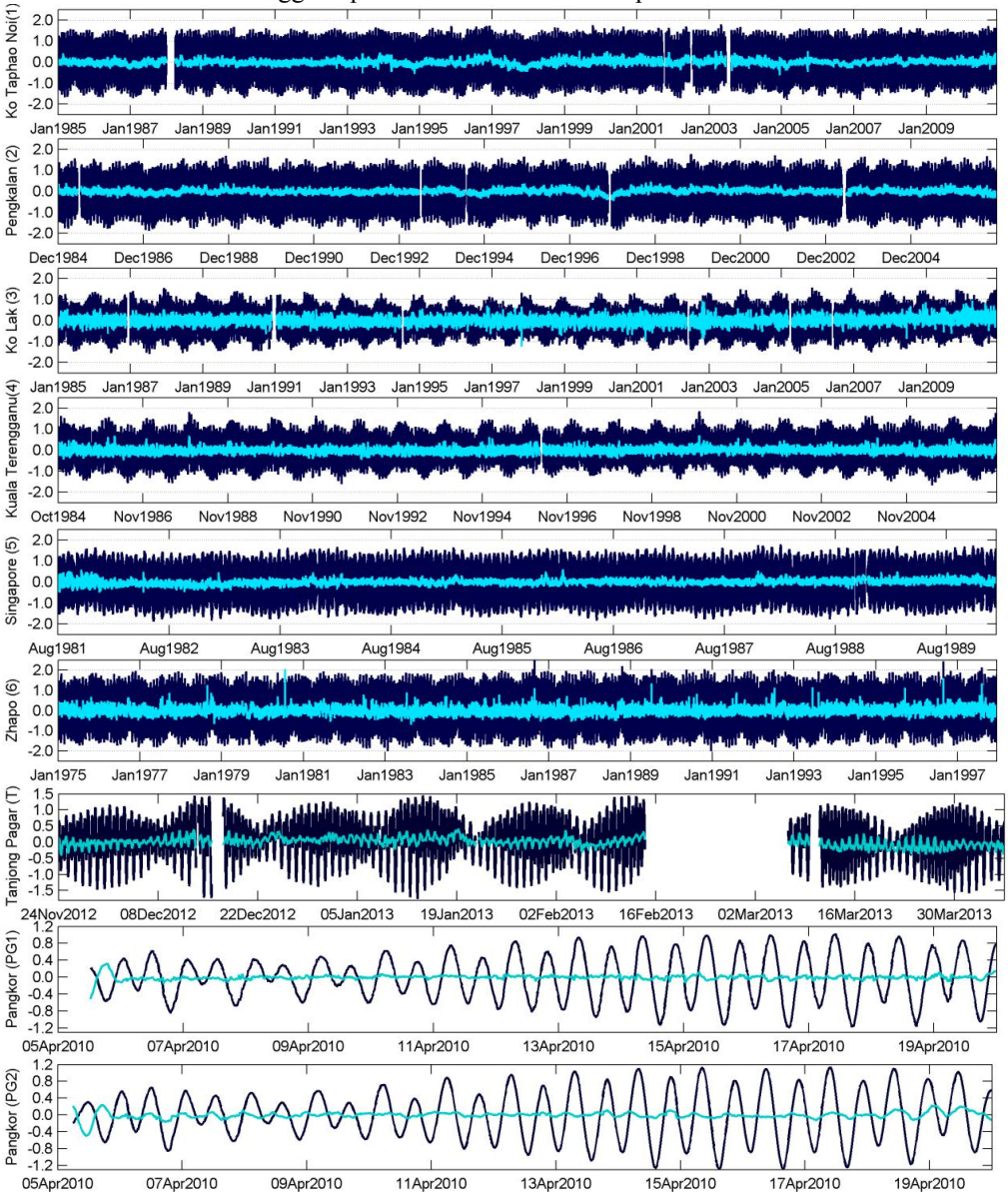

Figure 2; Sea level time series from the GLOSS, MEH and HYDEC tide gauges stations, in meters: astronomic tide (dark blue) and residual tide (light blue).

Regarding to the sea level anomaly (meteorological tide), the higher values were found in Ko Lak and Zhapo (in

light blue). Note that the time interval of the sea level under analysis was different according to the station and to the missing data: the first six images (GLOSS tide-gauges) present the largest time interval, compared with the following time series (for MEH and HYDEC tide-gauges).

Figure 3 represents all available data identified in Table 3 for the mean SLA'a. These change over the year and from station to station, essentially due to local MeteOcean conditions. It is clear that the monthly mean SLA's on the Malacca Strait are lower compared with South China Sea values: for Ko Taphao Noi and Pengkalan tide-gauges the differences between maximum monthly SLA'a are close to 20 cm, with maximums in May/November and minimums in February, while for Ko Lak and Kuala Terengganu the anomalies are around 40 cm, occurring between December and June (**Figure 3**, on the left).

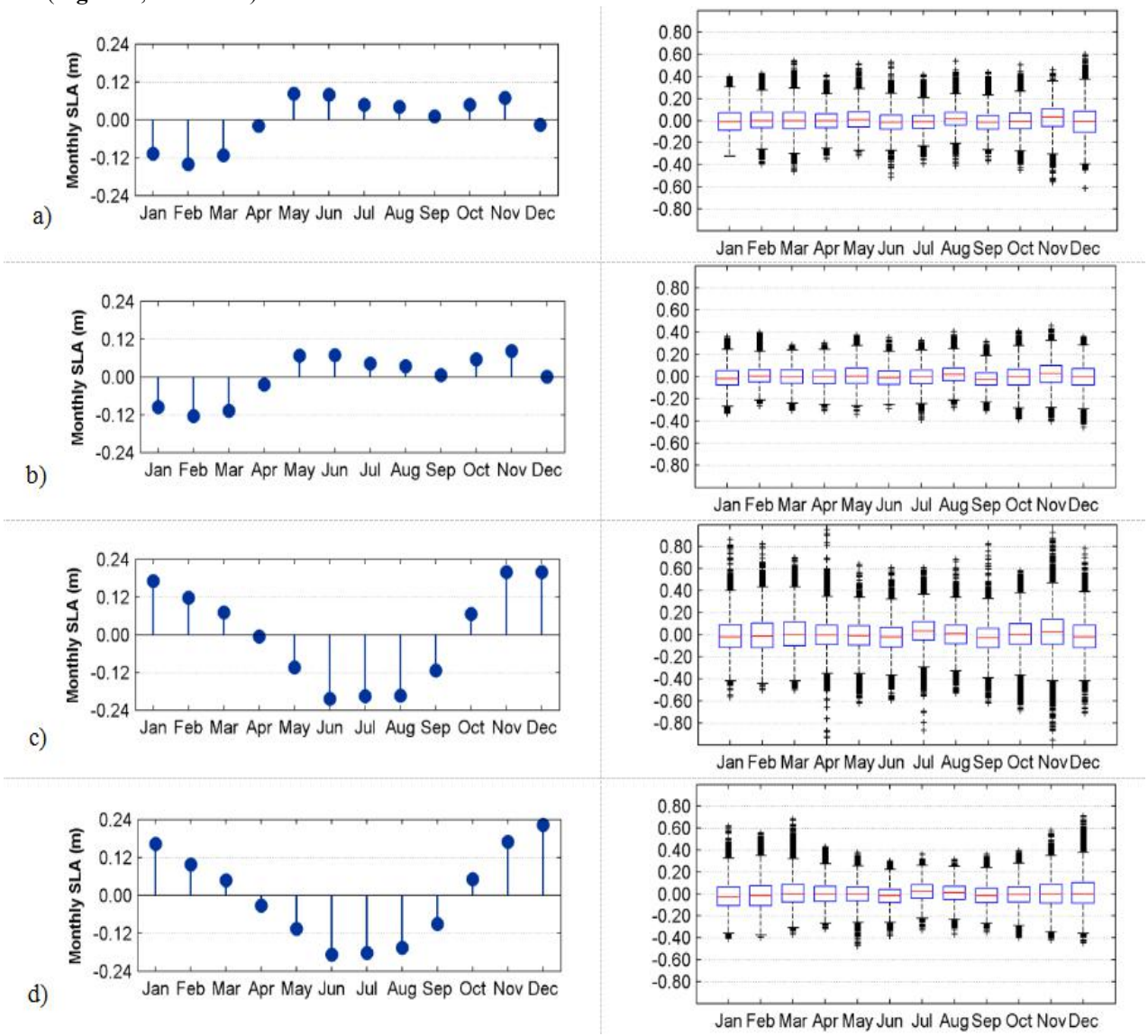

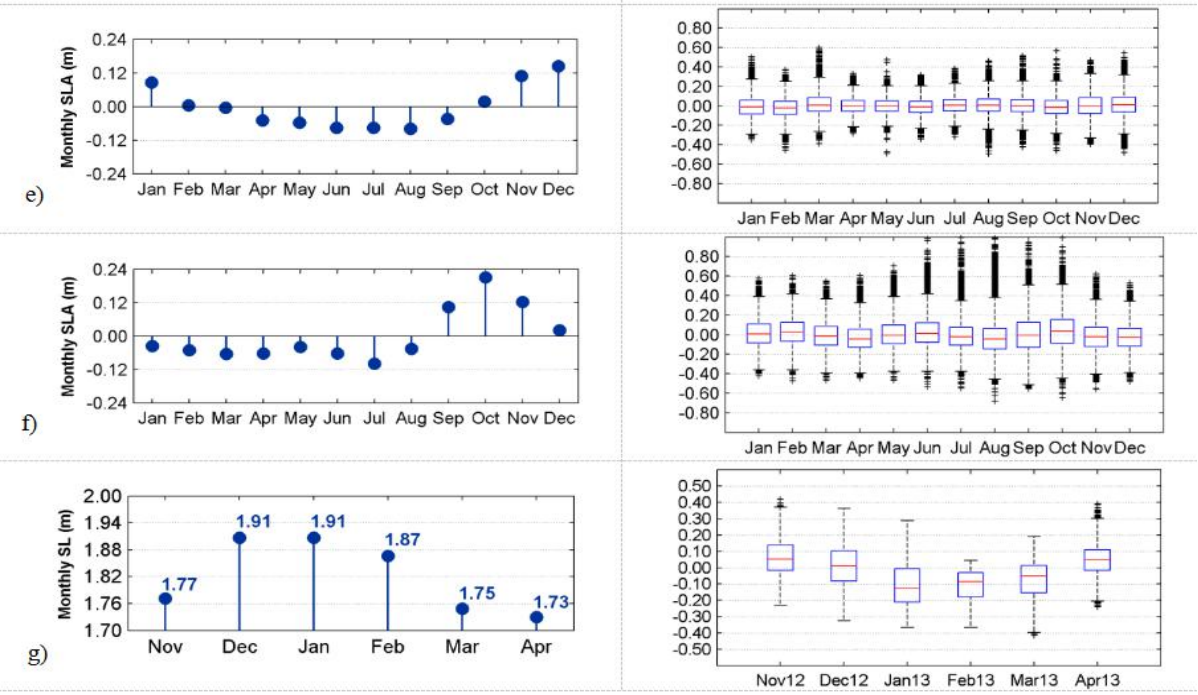

Figure 3; Monthly mean sea level anomaly (left) and box plot (right), including all available data of each tide gauge (Table 2), in meters, for (from top to bottom) Ko Taphao Noi, Pengkalan, Ko Lak, Kuala Terengganu, Singapore, Zhapo and Tanjong Pagar.

In the box plots of **Figure 3** (right), the central mark is the median, the edges of the box are the 25th and 75th percentiles, and the whiskers extend to the most extreme data not considered outliers. These are represented if they are larger than 1.5 times the difference between 75th and 25th percentile, at a distance from the 25th and 75th percentile corresponding to approximately 2.7 σ and 99.3 σ coverage to a normally distributed data. Those box plots were drawn using all the available sea level anomalies. The figure analysis reveals some important topics that should be referred: the occurrence of extreme SLA's is more common over the South China Sea comparing with the Malacca Strait; the northernmost stations (Kolak and Zhapo) present higher variations (higher box between the 25th and 75th percentile) and also the storm surges with higher amplitude, comparing with the other stations (more outliers); the stations southernmost in the South China Sea (Kuala Terengganu and Singapore) present a better relation with the occurrence of the monsoons, in agreement with the meteorological and ocean processes characteristic of the region. For Tanjong Pagar is presented the monthly mean sea level instead of the sea level anomaly (SLA), considering only few months of data were available for analysis. PG1 and PG2 are not shown in **Figure 3** because only a few days of data were available.

From the analysis of the SLA's distribution may be defined three classes of values (significant, very significant and highly significant for the SLA's percentiles of 95, 99, 99.9) and determined the maximum storm surge values (percentile 100). Table 4 presents storm surge levels for the tide gauges stations of the available GLOSS data. The higher values were found for Zhapo and Ko Lak, whereas for the Pengkalan station (on the Malacca Strait) was identified the lower values, comparing with the other stations.

Significant Levels	**Significant Storm Surge (95 %)**	**Very significant Storm Surge (99%)**	**Highly significant Storm Surge (99.9%)**	**Maximum Storm Surge (100%)**
Ko Tapthao Noi	0.1838	0.2795	0.3964	0.5923
Pengkalan	0.1611	0.2359	0.3257	0.4488
Ko Lak	0.2492	0.3758	0.5683	0.9509
Kuala Terengganu	0.1880	0.3037	0.4711	0.7095
Singapore	0.1723	0.2776	0.4263	0.5806
Zhapo	0.2642	0.4204	0.6914	2.0362

Table 4. Storm surge levels from GLOSS tide gauges stations, determined from all available observed data

4.2 Astronomic sea level analysis

To evaluate the accuracy of astronomic tide predictions from MSYM in each of the GLOSS, MEH and HYDEC tide-gauges, data sets have been subjected to harmonic analysis and the main constituents have been selected. The semidiurnal tidal constituents – M_2 and S_2 – are the major tidal harmonics for Ko Taphao Noi, Pengkalan and Pangkor, while the diurnal tidal constituents – K_1 and O_1 – dominate the tide in Ko Lak and Kuala Terengganu. The tide in the Malacca Strait is semidiurnal, in Singapore and Zhapo is mixed (mainly semidiurnal) and in Ko Lak is diurnal (all the form factors are detailed in Table 5).

Table 5. Form factor, type of tide, form factor and Relative HC for the main constituents for each tide-gauge and domain.

Tide gauges	Form factor (GLOSS)	Type of Tide	Validated Level	Form factor (MSYM)	Relative HC (%)				
					M_2	S_2	K_1	O_1	M_4
Ko Taphao Noi	0.15	Semidiurnal	L1	0.14	16	25	13	30	413
			L2	0.14	15	20	9	32	236
Ko Lak	11.61	Diurnal	L1	12.50	96	184	31	17	394
			L2	15.08	74	139	36	21	319
Kuala Terengganu	1.96	Mixed (Diurnal)	L1	3.05	48	55	36	24	210
			L2	3.10	48	54	38	25	191
Pengkalan	0.23	Semidiurnal	L1	0.23	21	30	7	173	139
			L3	0.29	15	17	15	239	113
Zhapo	0.82	Mixed (Semidiurnal)	L1	0.69	27	19	3	4	73
Tanjong Pagar	0.59	Mixed (Semidiurnal)	L4	0.57	6	15	10	9	181
Pangkor PG1	0.28	Mixed (Semidiurnal)	L3	0.21	19	81	28	47	48
Pangkor PG2	0.24	Semidiurnal	L3	0.25	13	52	45	218	215

MSYM model was run for the four levels of grid nesting (L1 to L4) and the results were compared with values of L1 and with the smaller level that each station can include. **Figure 4** and **Figure 5** present the amplitude and phase of the major tidal harmonics of all tide-gauges under analysis (diurnal: Q_1, O_1, P_1, K_1; semidiurnal: N_2, M_2, S_2, K_2; quadridiurnal: M_4). The Singapore station is out of the model domain, so its validation wasn't performed. In general, the MSYM results reveal an agreement between predictions and observations. To quantify the model's accuracy, the Relative HC of each constituent is computed and presented for the four main harmonics in the Table 5. For the tide-gauges in which two levels are compared, the Relative HC decreases as the model resolution increases, with the exception of O_1 in Ko Taphao Noi and of the diurnal constituents in Ko Lak, Kuala Terengganu and Pengkalan. However, an improvement in M_4 accuracy is observed for all tide-gauges as the resolution increases, as expected, since the generation of this constituent is dependent on the bathymetry (**Figure 1**). The higher amplitude harmonics predictions are overestimated for each tide-gauge and in general, except for the M_2 constituent at PG2. The higher phase differences were found for M_4 constituent for most tide-gauges (although the amplitude of this constituent is low).

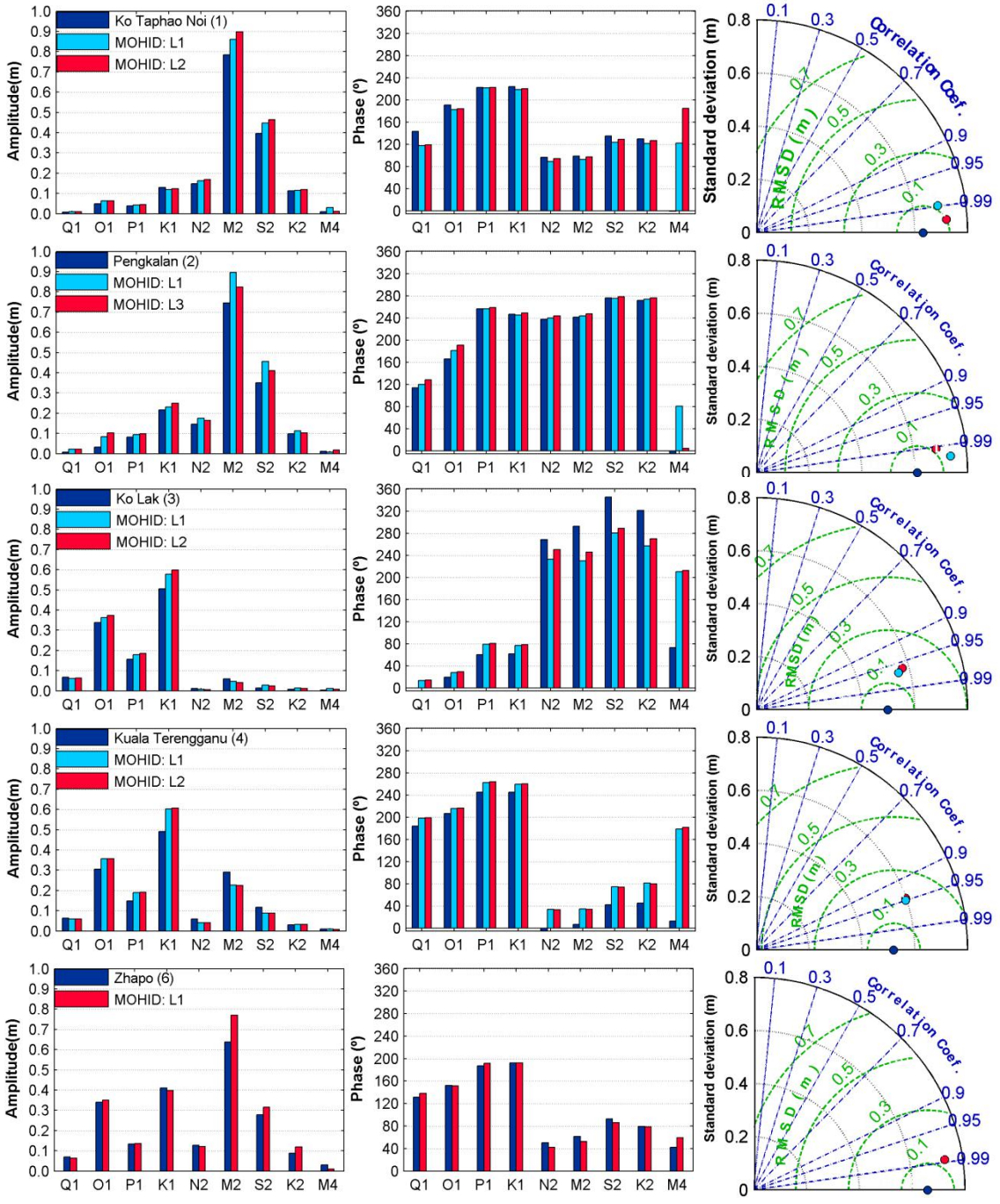

Figure 4; Amplitude in meters (left), phase in degrees (center) of the main constituents separated with t_tide function and Taylor Diagram (right) for (from top to bottom) Ko Taphao Noi (1 – corresponding number marked in the Figure 1); Pengkalan (2); Ko Lak (3); Kuala Terengganu (4); Zhapo (6). Period is between 17th of December of 1988 and 23rd of December of 1989.

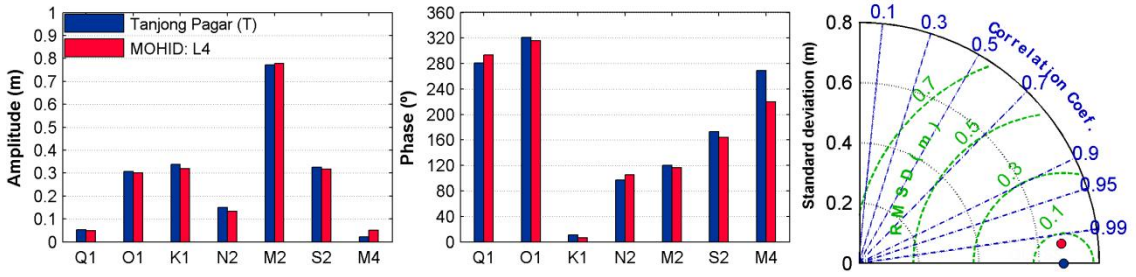

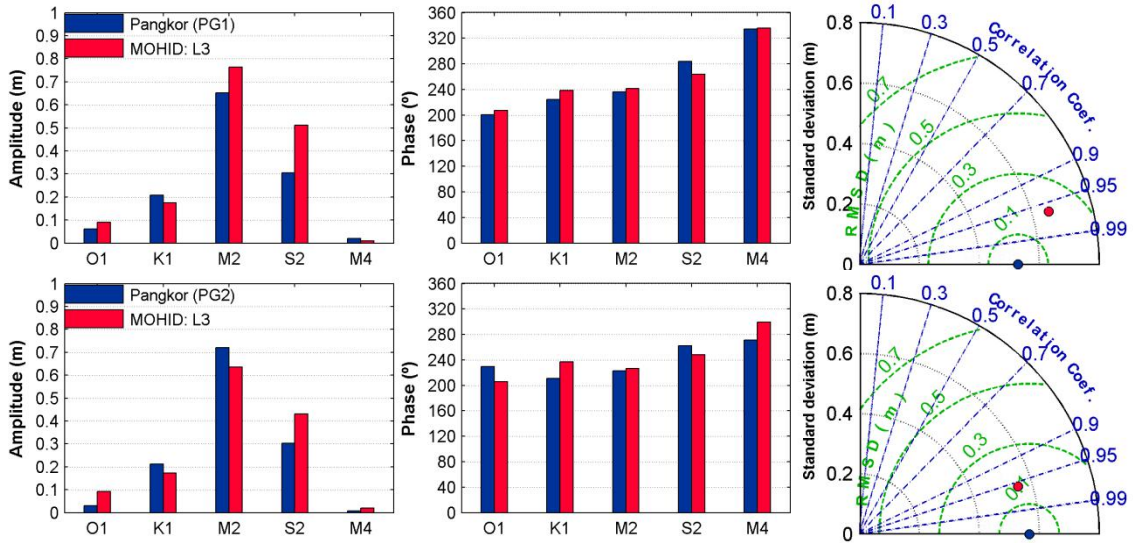

Figure 5; Amplitude in meters (left), phase in degrees (center) of the main constituents separated with t_tide function and Taylor Diagram (right) for (from top to bottom) Tanjong Pagar (T) and Pangkor (PG1 and PG2). Period is from 24th of November of 2012 to 6th of April of 2013 for Tanjong Pagar and from 5th April to 19th of April of 2010 for both Pangkor tide gauges.

The Correlation coefficient, RMSE' and the Relative Error were also calculated for each station, and are displayed in the Taylor Diagrams presented in **Figure 4** and **Figure 5** (right). Analysing these error measures (for both domains), it was found that the astronomic tide is better reproduced for the tide-gauges in the Malacca Strait, comparing with the tide-gauges in the east coast of Peninsular Malaysia. Even though the Correlation Coefficient is close to 1 (equal to and above 0.95, when considering all tide-gauges) indicating a good correlation between the observations and predictions, it is important to take the RMSE' into account. While the RMSE' for Ko Taphao Noi, Pengkalan, Zhapo and Tanjong Pagar is between 10 and 15 cm, corresponding to a relative error around 4% (and even smaller for predictions using a higher horizontal resolution), for Ko Lak, Kuala Terengganu and Pangkor the RMSE' is between 15 and 20 cm (and higher for higher horizontal resolutions). Overall, the best astronomic tide model predictions were found for the Tanjong Pagar.

4.3 Meteorological analysis

Even though the astronomical tide has larger amplitude, the meteorological tide also has an important contribute for the sea level. Thus, this part of the study is focused in the analysis of the meteorological tide for Tanjong Pagar (T) and Pangkor (PG1 and PG2) tide-gauges, which were the only tide-gauges located in areas where the model also included meteorological forcing.

As previously described, the South China Sea is a very dynamic region (with consequences on the sea level patterns), which is affected by monsoons which dominate the larger-scale sea level dynamics. The typical monsoons during the period analysed for Tanjong Pagar are from NE, and the higher frequencies of the SLA's show storms occurrence.

Daily mean pressure and wind fields at 10 m were computed for the region using three-hourly data (from GFS). Monthly means were calculated from this data and plotted in **Figure 6** for December, January, February and March, from left to right, for pressure and wind, top and bottom respectively. The pressure monthly means display higher pressures over the China region, especially in January (monthly maximum of about 1028 hPa). On the other hand, the wind monthly means show a predominance of the highest wind speeds along the Taiwan (25.05º N; 121.53º E) – Singapore (1.29º N; 103.85º E) axis, in agreement with previous studies (Choon *et al*., 2006; Tkalich *et al*., 2013; Chen *et al*., 2011). January presents the highest wind speed mean (near to 14 m/s, offshore of Vietnam). According to Tkalich *et al*. (2013), the NE monsoon climatology and extreme wind, when aligned along the longest Taiwan–Singapore axis,

produce the strongest positive SLA's in the Tanjong Pagar tide-gauge region.

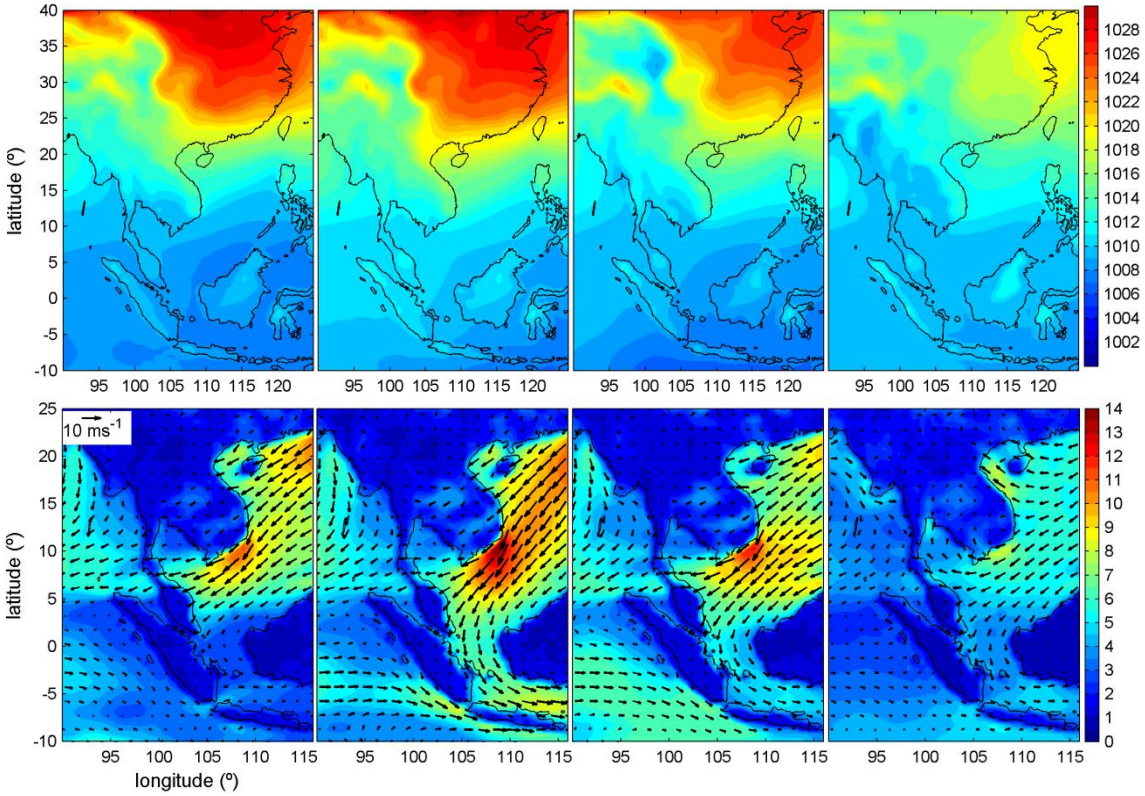

Figure 6; Monthly surface pressure means, in hPa, (top) and wind speed and direction (colour and vector scale, respectively) at 10 m, in m/s, (bottom), for December, January, February and March, from the left to the right.

The SLA's obtained by filtering the astronomical tide from observations and predictions are shown in **Figure 7.** From the analysis of this figure are found some differences between SLA's for observations and predictions, revealing that the model is unable to simulate some anomalies, underestimating its values, as suggested by the histograms in Figure 7 (left). The correlation, the RMSE and the standard deviation are about 0.72, 0.099 m and 0.141 m, respectively.

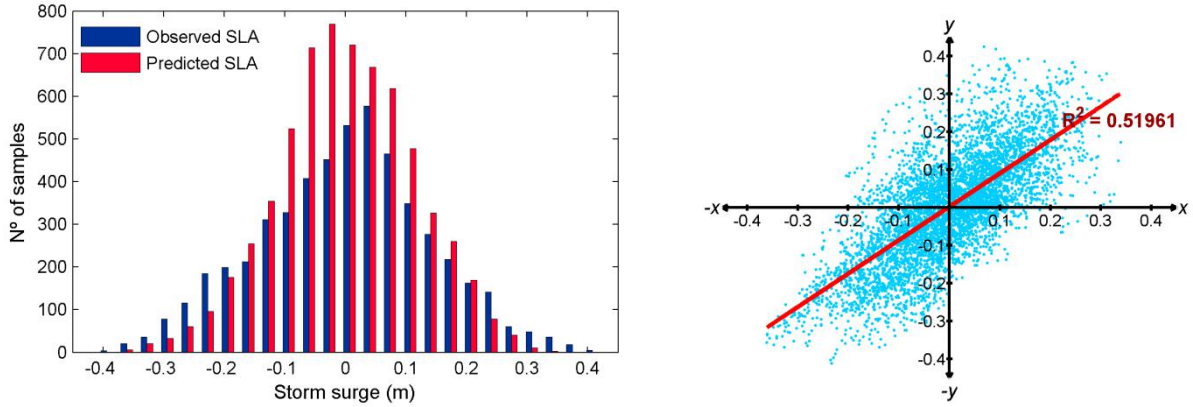

Figure 7; Sea level anomalies histogram for Tanjong Pagar (bottom left) and correlation (bottom right) between the sea level anomalies from observed time series (yy axis) and predicted time series (xx axis).

The highest positive SLA's are mainly identified in December and January, with amplitudes near 30 cm, and are generated by NE winds over the South China Sea with intensity near 18 ms^{-1}. In spite of the predominant NE winds, negative SLA's were also identified in February, resulting from weak winds with a change of direction into SW. Regarding the wind fields, the climatology of the wind at 10 m showed more intense winds offshore of Vietnam and in a region north of Vietnam, which is also the area where the correlation between SLA's in Tanjong Pagar and the wind

speed is higher.

In order to evaluate this relationship, was computed the correlation coefficient between the gridded wind (50 by 50 km from GFS) along the Singapore-Taiwan axis (**Figure 8**, left) and pressure (**Figure 8**, right) data sets and the SLA's in the Tanjong Pagar, for the entire MSYM (L1) domain. The highest correlations with the wind along the Taiwan-Singapore axis were found between 10-20°N and 107-113°E, with a maximum value of 0.561. Regarding the pressure, the pattern for the maximum correlation coefficient was similar; however, it appears over the China and Taiwan region. Therefore, higher pressures over the China region induce anomalies in the Singapore Strait, and the occurrence of storm surges can be related with the meteorological conditions in this region. The maxima of the correlation coefficients were determined from **Figure 8** and their time series (pressure and wind) were plotted in **Figure 9.** These results show that an increase in the pressure (over the China region) causes an increase of SLA's; on the other hand, changes in wind direction and speed near Vietnam (at around 8–18° N and 107–113°E) induce variations on the SLA's.

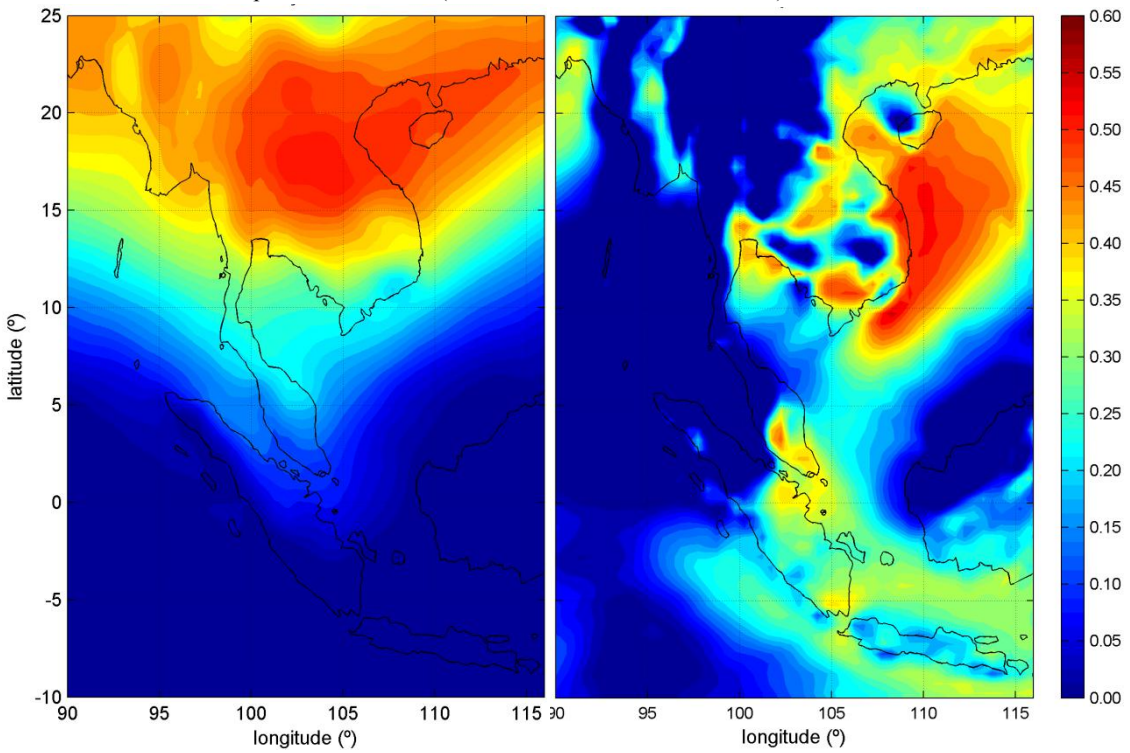

Figure 8; Spatial distribution of the correlation coefficient between the sea level anomalies in Tanjong Pagar and the pressure along the Taiwan-Singapore axis (left) and the wind speed along the Taiwan-Singapore axis (right).

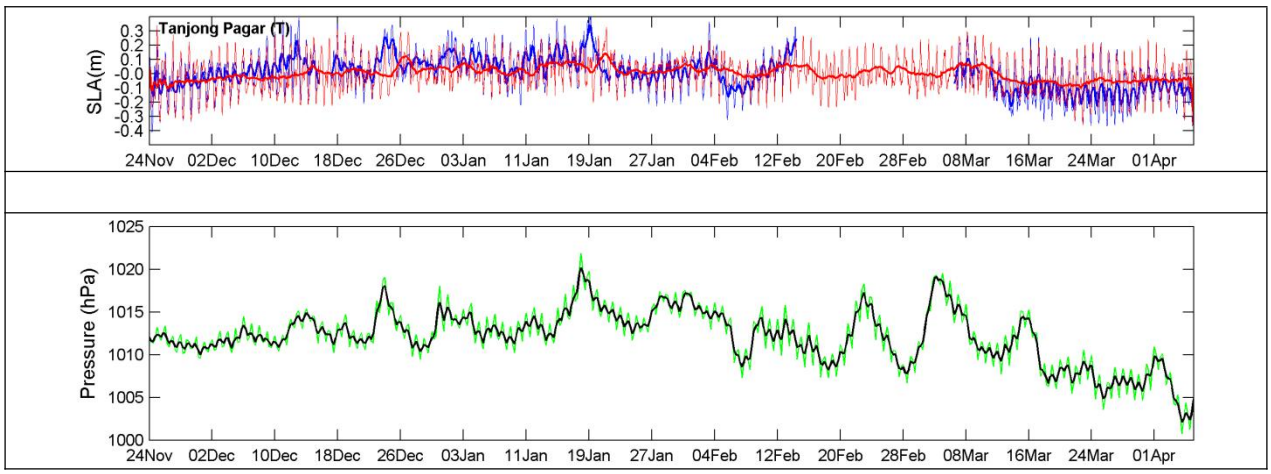

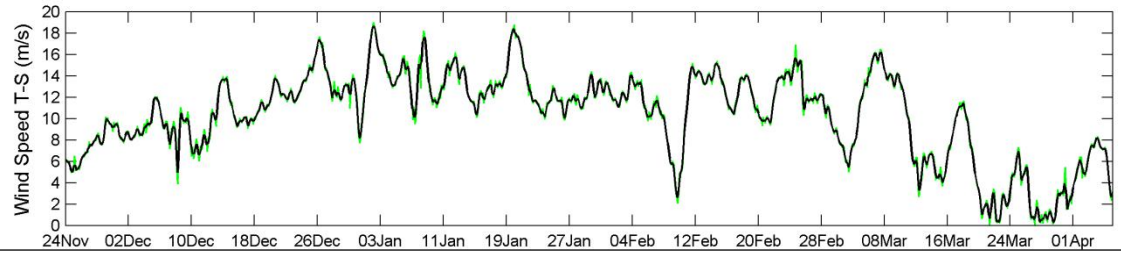

Figure 9; Sea level anomalies for predicted (red) and observed (blue) data for Tanjong Pagar (top). Pressure (middle) and wind speed (bottom) along the Taiwan-Singapore axis for the locations with the highest correlation coefficients determined from **Figure 8.**

Regarding the meteorological tide in Pangkor (PG1 and PG2), SLA's of the order of 10–20 cm were found (**Figure 10**). The typical wind speed in the Malacca Strait is not as high as that found over the South China Sea, and significant wind events were not found during this time interval. Consequently, the differences between observations and predictions found in Pangkor tide-gauges may be essentially induced by inaccuracies in model predictions for the amplitude and phase of the major harmonics, which are strengthened during the neap tide.

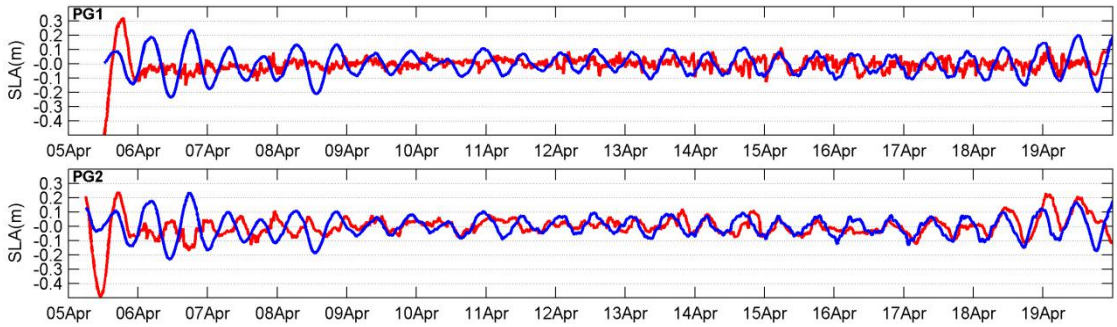

Figure 10; Sea level anomalies determined from predicted (red) and observed (blue) data for PG1 (top) and PG2 (bottom).

5. Conclusions

The region of the South China Sea, entangled between the Pacific Ocean and the Indian Ocean, is characterized by a very complex tidal behaviour driven by the tidal propagation from the two oceans. There is a strong variation of the bathymetry from the deep sea basins to the shallow areas, where the NE monsoon and SW monsoon dominate the large-scale sea level dynamics. Consequently, the consideration of MeteOcean processes is important when major developments are proposed in estuarine or coastal modelling. In this context, a numerical model was developed for this region following a downscaling approach using four levels of grid nesting, and special attention to the Malacca and Singapore Strait region (MSYM). After a brief characterization of the tidal behaviour in this region, a comparison between observed and predicted astronomic tides was performed for the region. The results demonstrated that the best fit between predictions and observations was found for Ko Taphao Noi and Tanjong Pagar, with a RMSE' around 10 cm for spring tide with amplitude higher than 3 m and a Relative Error of about 4%. The worst predictions were found for Kuala Terengganu and Pangkor (RMSE' near 20 cm).

The meteorological tide was also analysed for three tide-gauges: one in the Singapore Strait (Tanjong Pagar) and two in the Malacca Strait. Due to the geomorphological configuration of the Sunda Shelf, SLA's are amplified by the wind stress forcing, and depending on the wind speed and direction over the South China Sea, the Singapore Strait could experience positive or negative SLA's. The analysis of the spatial distribution of the wind revealed that the positive SLA's are mainly coincident with periods of strong winds over the South China Sea, along the Taiwan-Singapore axis. The climatology of the wind at 10 m showed more intense winds offshore Vietnam and in a region north of Vietnam, which comprises the area where the correlation between SLA's and the wind speed is higher

and includes the location of in Tanjong Pagar. On the other hand, the SLA's for the Pangkor tide-gauge are in the order of 10 – 20 cm, for both tide-gauges. Part of the residual tide is still due to inaccuracies in the astronomic tide, which could not be completely separated due to the limited time interval of 15 days (this short period of time can introduce errors in the amplitude and phase calculations of the main harmonics).

In summary, the MSYM sea level predictions show different accuracies according to the site analysed induced by the region's complexity and by the local influence of MeteOcean factors. In general, it was found a good model reproduction for most of the area simulated. However, for the Singapore Strait were identified significant discrepancies between predicted and observed sea level, which are most of the times associated with events of meteorological tide induced by surface wind stress and atmospheric pressure gradients. For the Malacca Strait were also found important differences, mainly related with model limitations in reproducing the local astronomical tide (amplitude and phase of the main constituents).

References

1. Azmy A. R., Y. Isoda, T. Yanagi. Sea Level Variations due to Wind around West Malaysia. Memoirs of the Faculty of Engineering. Ehime University, 1991, XII: 148–161.
2. Akdag C. Tidal analysis of the South China Sea. Delft University of Technology, Delft Hydraulics, 1996: 85.
3. Assilzadeh H., Maged M., Mansor S., Mohamed M. Application of Trajectory Model, Remote Sensing and Geographic Information System (GIS) for Oil Spill Contingency Planning in Straits of Malacca. Proceedings of the International Symposium on Digital Earth Science Press, 1999.
4. BraunschweigF. Generalização de um modelo de circulação costeira para albufeiras, MSc. Thesis, Instituto Superior Técnico, Technical University of Lisbon, 2001.
5. Braunschweig F., Martins F., Chambel P., Neves R. A methodology to estimate renewal time scales in estuaries: The Tagus estuary case. Ocean Dyn, 2003; 53(3): 137–145.
6. Camerlengo A., Demmler M. I. Wind-driven circulation of Peninsular Malaysia's eastern continental shelf. Sci. Mar., 1997; 61(2): 203–211.
7. Chanut J., Galloudec O. L., Léger F. Towards North East Atlantic Regional modelling at 1/12° and 1/36° at Mercator Ocean. Mercator Ocean Quarterly Newsletter, 2008.
8. Chen H., Wei J., Tkalich P., Malanotte-Rizzoli P. The Various Constituents of the Circulation in the Singapore Strait Region: Tidal, Wind and Eddy driven Circulations and Their Relative Importance. In Papers of the 20th International Offshore and Polar Engineering Conference, ISOPE-2010, Beijing, China, June 20–26, 2010.
9. Chen H., Tkalich P., Malanotte-Rizzoli P. Data Analysis and Numerical Modelling of Sea Level Anomalies in the South China Sea. Proceedings of the 34th World Congress of the International Association for Hydro-Environment Research and Engineering: 33rd Hydrology and Water Resources Symposium and 10th Conference on Hydraulics in Water Engineering. Barton, A.C.T.: Engineers Australia, 2011: 519–526.
10. Choon L.K, Lye K.H., Juneng L., Tanggang, F. Simulation of circulation and storm surge in South China Sea. International Conference on Environment 2006 (ICENV 2006), 13–15 November 2006, Penang, Malaysia.
11. Dias J.M. Contribution to the study of the Ria de Aveiro hydrodynamics. Ph.D. Thesis, University of Aveiro, Portugal, University of Aveiro, 2001: 288.
12. Kurniawan A., Ooi S.K., Hummel S., Gerritsen H. Sensitivity analysis of the tidal representation in Singapore regional waters in a data assimilation environment. Ocean Dyn, 2011; 61(8): 1121–1136.
13. Keller G.H., Richards A.F. Sediments of the Malacca Strait, Southeast Asia. J Sediment Petrol, 1967; 37(1): 102–127. doi: 10.1306/74D7166D-2B21-11D7-8648000102C1865D.
14. Leitão P. Modelo de dispersão lagrangeano tridimensional – dissertação de mestrado. Instituto Superior Técnico, Universidade Técnica de Lisboa, Lisboa, 1996.
15. Lyard F., Lefèvre F., Letellier T., Francis O. Modelling the global ocean tides: a modern insight from FES2004, Ocean Dyn, 2006; 56(5–6): 394–415.
16. Martins F., Leitão P., Silva A., Neves R. 3D modelling in the Sado estuary using a new generic vertical discretization approach. Oceanologica Acta, 2001; 24 (1): 51–62. doi: 10.1016/S0399-1784(01)00092-5.
17. Montero P., M. Gómez-Gesteira, J. J. Taboada, M. Ruiz-Villarreal., A. P. Santos, R. R. Neves, R. Prego, V. Pérez-Villar. On residual circulation of Vigo Ría using a 3D baroclinic model, Boletín Instituto Español de Oceanografía, Bol. Inst. Esp. Oceanogr, 1999; 15(1–4): 31–38.
18. Pawlowicz R., Beardsley R., Lentz S. Classical Tidal Harmonic Analysis including Error Estimates in MATLAB using T_Tide. Computers and GeoSciences, 2002; 28(8): 929–937. doi: 10.1016/S0098-3004(02)00013-4.
19. Rizal S., Setiawan I., Iskandar T., Ilhamsyah Y., Wahid M., Musman M. Currents Simulation in the Malacca Straits by Using Three-Dimensional Numerical Model. Sains Malays, 2010; 39(4): 519–524.
20. Stewart R. H. Introduction to Physical Oceanography. Department of Oceanography, Texas A&M University,

2008.
21. Tkalich P., Huda M. K., Gin K. . A multiphase model of oil spill dynamics. Proceedings of the XXVII IAHR Congress 22–27 August 1999, Graz, Austria..
22. Tkalich P., Babu M.T., Vethamony P. Technical Note: Mean sea level variation in the Singapore Strait from long-term tide data. Ocean Sci., 2012; 9(3): 2255–2271. doi:10.5194/osd-9-2255-2012.
23. Tkalich P., Vethamony P., Babu M.T., Malanotte-Rizzoli P. Storm surges in the Singapore Strait due to winds in the South China Sea. Natural Hazards, 2013; 66(3): 1345–1362. doi: 10.1007/s11069-0211-8.
24. Vaz N., Dias J.M. Hydrographic characterization of an estuarine tidal channel. Journal of Marine Systems, 2008; 70 (1–2): 168–181. doi: 10.1016/j.jmarsys.2007.05.002.
25. Villarreal M.R., Montero P., Taboada J.J., Prego R., Leitão P.C., Péres-Villar V. Hydrodynamic model study of the Ria de Pontevedra under estuarine conditions. Estuar Coast Shelf Sci, 2002; 54(1): 101–113. doi: 10.1006/ecss.2001.0825.
26. Wei J., Zeng H., Ooi B.H., Dao M.H., Cho W. Multi-layer model simulation and data assimilation in the Serangoon Harbor of Singapore. Proceedings of the International Offshore (Ocean) and Polar Engineering Conference, 2010.
27. Wang B., R. Wu, K. M. Lau. Interannual variability of Asian summer monsoon: Contrast between the Indian and western North Pacific-East Asian monsoons. J. Climate, 2001; 14(20): 4073–4090. doi: 10.1175/1520-0442(2001)014<4073.